SEEQUENT

# GeoStudio Example File

# Progressive Failure of a Cut in London Clay due to Strain Softening

To see the latest GeoStudio learning content, visit Seequent Learning Centre and search the catalogue for “GeoStudio”.

# Introduction

Potts et al. (1997) used a finite element analysis to explore a link between strain softening and delayed failures of old railway slopes cut into stiff plastic clays. Strain softening causes a soil's strength to reduce from a peak to residual state. The strength loss does not occur simultaneously along a potential rupture zone because the rate of softening is linked with the magnitude of shear straining. As a result, the failure is progressive in the sense that the rupture surface propagates through the soil profile over time. SIGMA/W's coupled formulation, in combination with the Mohr-Coulomb Hardening/Softening, was used to simulate this case history and therefore to explore the progressive failure mechanism.

# Numerical Simulation

SIGMA/W's coupled stress-strain and water transfer formulation (i.e. Consolidation analysis) was used to simulate the excavation of a slope cut into a strain-softening, stiff, plastic clay. A coupled analysis was also used to simulate the equilibration of the pore-water pressures and resulting deformations that occurred once the excavation was complete (i.e. swelling phase).

The behavior of the strain softening Brown London Clay was simulated using the Mohr-Coulomb Hardening/Softening model. Table 1 summarizes the inputs used to characterize the stiffness, strength, and hydraulic properties of the clay. Young's modulus was varied with y-coordinate, not mean effective stress as was done by Potts et al. (1997). Potts et al. (1997) established the peak and residual effective strength properties from ring shear tests and back-analysis. The deviatoric plastic strain $\varepsilon_q^p$ at the onset of softening is 3% while that required to reach the residual condition is 12% (Potts et al. 1997). Figure 1 and Figure 2 show the input softening functions for the effective friction angle and cohesion, respectively. [Note: the deviatoric strain invariant $\varepsilon_q = \varepsilon_J/\sqrt{3}$ where $\varepsilon_J$ is the deviatoric strain invariant used by Potts et al. (1997)]. The saturated only model was used to represent the hydraulic properties of the London Clay. A hydraulic conductivity of 5.0E-10 m/s was deduced from graphs of the spatially variable profiles of hydraulic conductivity presented by Potts et al. (1997).

**Table 1. Soil properties for the soft clay.**

| Parameter | Value |
|---|---|
| Young's modulus (kPa) | Variable (min 4000 kPa) |
| Poisson's ratio ($\nu$): | 0.2 |
| Unit Weight ($\gamma$; kN / m$^3$): | 18.8 |
| $K_{sat}$ (m/s) | 5.0 x $10^{-10}$ |
| Earth Pressure Coefficient | 1.5 |
| Peak effective friction angle | 20 |
| Peak effective cohesion (kPa) | 7 |
| Deviatoric plastic strain at peak | 3% |
| Residual effective friction angle | 20 |
| Residual effective cohesion (kPa) | 7 |
| Deviatoric plastic strain at residual | 12% |

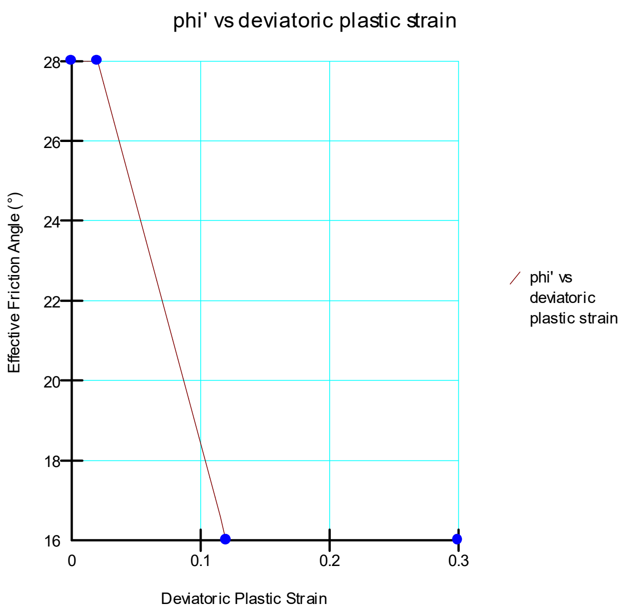


**Figure 1. Effective friction angle versus deviatoric plastic strain.**

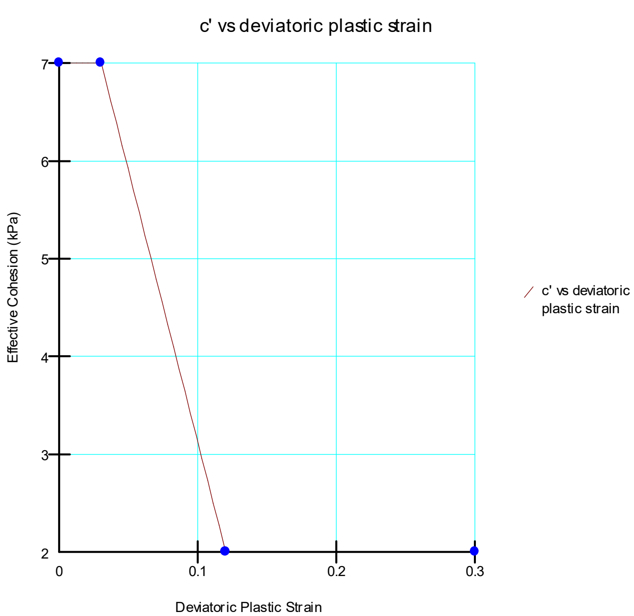


**Figure 2. Effective cohesion versus deviatoric plastic strain.**

The analysis tree and finite element domain and boundary conditions are shown in Figure 3 and Figure 4, respectively. The initial *in situ* stresses were established assuming hydrostatic pore-water pressure conditions with the water table 1 m below ground surface. The initial stresses were established with an earth pressure coefficient of 1.5 (Table 1). The excavation was 10 m deep with 3:1 side slopes. The excavation phase was simulated by deactivating 4 regions of 1 m thickness and three regions of 2 m thickness. Each excavation phase was simulated using one time step of duration 1 day, resulting in the excavation being completed in 7 days. Potts et al. (1997) modelled the excavation sequence over a 3 month period; however, almost no swelling occurs during this time, making it reasonable to complete this part of the simulation more rapidly.

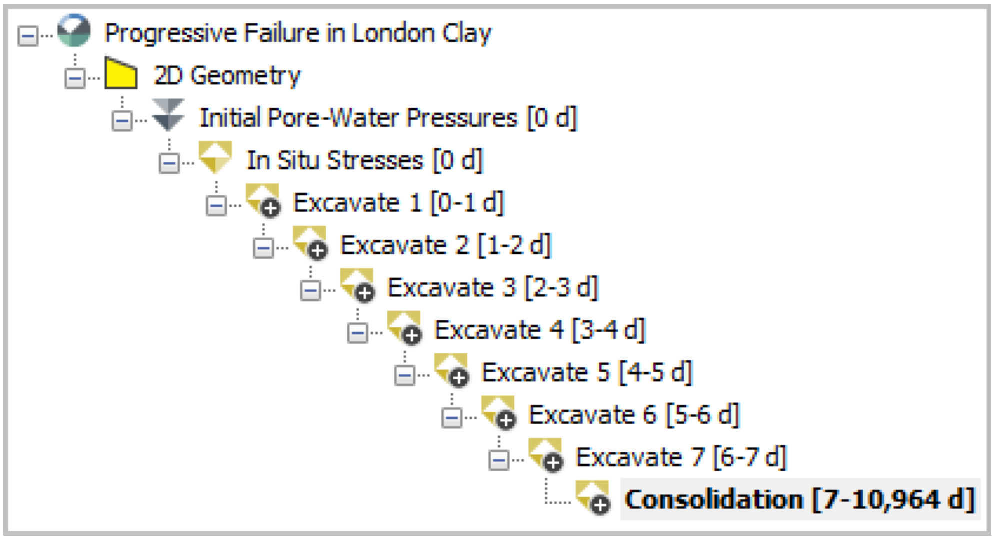


**Figure 3. Analysis tree for the Project.**

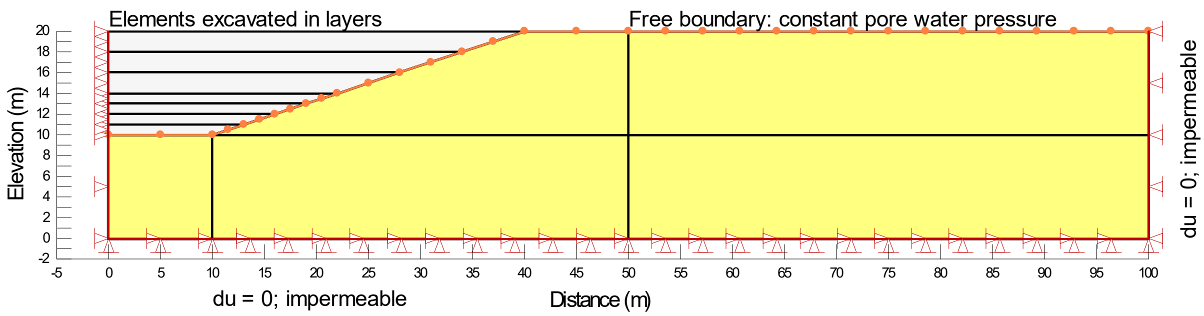


**Figure 4. Finite element mesh and boundary conditions.**

The swelling phase was simulated for approximately 30 years (11,000 days) using an exponential time sequence. During the swelling phase, the pore-water pressure was maintained at -10 kPa along the surface boundary. The upper hydraulic boundary condition represents the average measured surface pore-water pressure (Potts et al, 1997).

# Results and Discussion

Progressive failure refers to the non-uniform mobilization of shear strength along a potential rupture surface. In the case of a cut slope, the area near the toe at the base of the excavation may have mobilized the peak shear strength by the end of construction. The rupture surface will propagate further into the slope once the excavation is complete and the pore-water pressures begin to recover (mean effective stresses decrease); that is, more of the domain will reach peak strength. At the same time, the already failed soil experiences an ever increasing amount of shear strain that can cause a loss of strength. This mechanism is referred to as strain-softening. At collapse, part of the rupture surface will have a post-peak shear and perhaps approach a residual strength, while part of the rupture surface will not even have formed (Potts et al., 1997). Therefore, the average strength of the soil along the rupture surface at collapse must be less than the peak strength, but greater than the residual strength.

## GeoStudio Example - Progressive Failure of a Cut in London Clay due to Strain Softening

A rapid excavation into low hydraulic conductivity clay unloads the soil and causes a tendency for volumetric expansion. The tendency for volumetric expansion is offset by a reduction in the pore-water pressures, resulting in a nearly undrained response. The extent of the depression in the phreatic surface as a result of the unloading is rather dramatic (Figure 5). A total of 10 m of soil was removed, causing a decrement in the pore-water pressure just beneath the base of the excavation of over 120 kPa (Figure 6). Over time the soil affected by the excavation takes in in water, causing a reduction in the mean effective stresses, which is reflected in volumetric expansion (i.e. swelling). The reduction in mean effective stress in some areas of the soil domain can bring the stress states onto the failure surface. The overall collapse of the slope is therefore delayed by the time required for pore-water pressure equilibration. The pore-water pressures are still recovering after 8000 days (about 22 years; Figure 6).

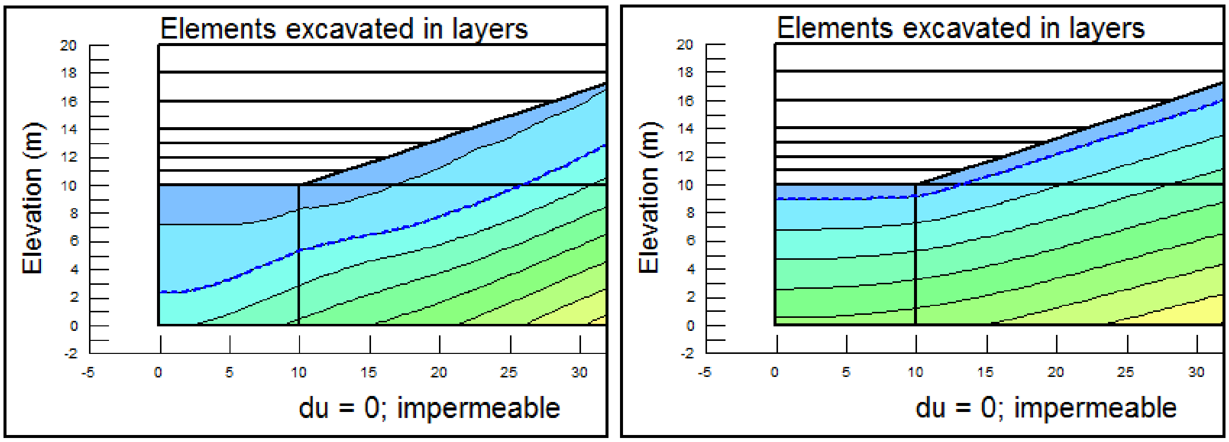


**Figure 5. Piezoemetric lines at the end of construction (left) and at the end of the swelling phase (right).**

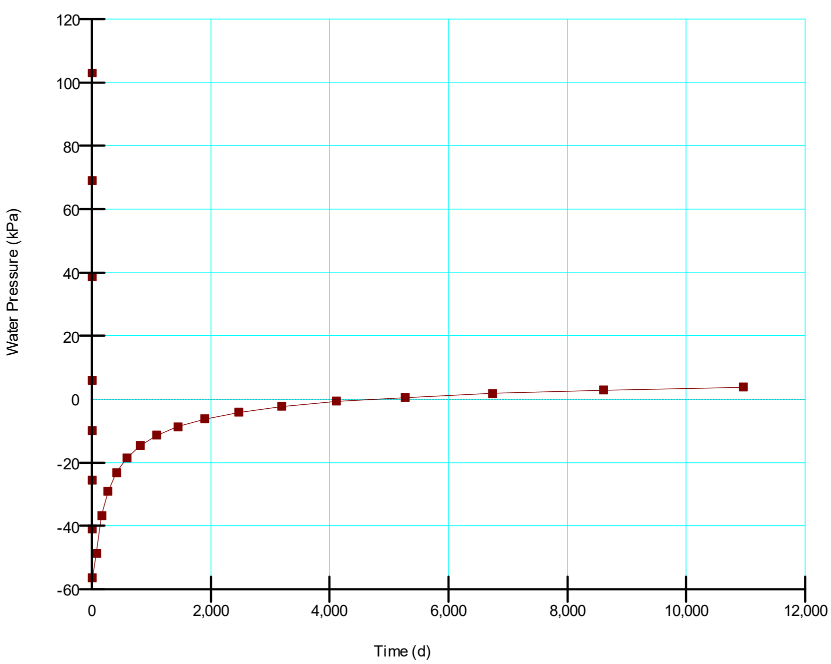


**Figure 6. Pore water pressure response at Elevation 8.5 m along the centerline of the excavation.**

According to the progressive failure mechanism theory, the strength for soils that have been heavily sheared is between the peak and residual values. The Mohr-Coulomb

Hardening/Softening model reduces the strength in accordance with strength functions (Figure 1 and Figure 2). The Mohr-Coulomb Hardening/Softening model captures a progressive failure in the truest sense because the strength varies along the rupture zone in a manner that is commensurate with accumulated plastic shear strains. Figure 7 presents contours of plastic deviatoric strain after 3 years (top), 18.5 years (middle), and 30 years (bottom). Figure 8 shows the plastic states at the same elapsed times. A rupture zone is clearly propagating towards the crest as swelling occurs (Figure 7). The rupture zone is fully formed by 30 years. The plastic states (Figure 8) depict which gauss regions have stress states on the failure surface; however, unlike Figure 7 it is difficult to discern which parts of the domain might be experiencing strain softening because there is no information about the dominant mode of deformation (i.e. volumetric or deviatoric). Having stated that, the global rupture zone is clearly demarcated by the plastic states at an elapsed time of 30 years (Figure 8).

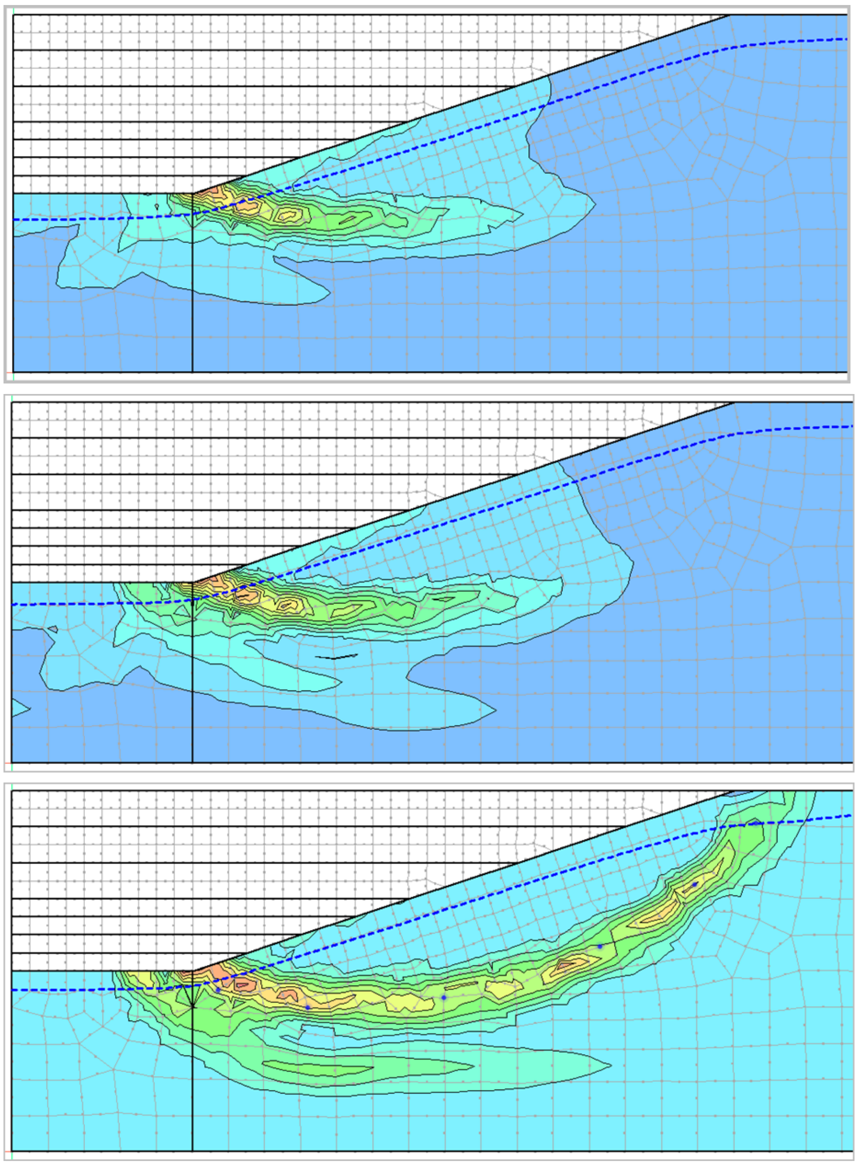

Figure 7. Plastic deviatoric strain contours after 11.3 year (top), 18.5 year (middle), and 30 year (bottom).

GeoStudio Example - Progressive Failure of a Cut in London Clay due to Strain Softening

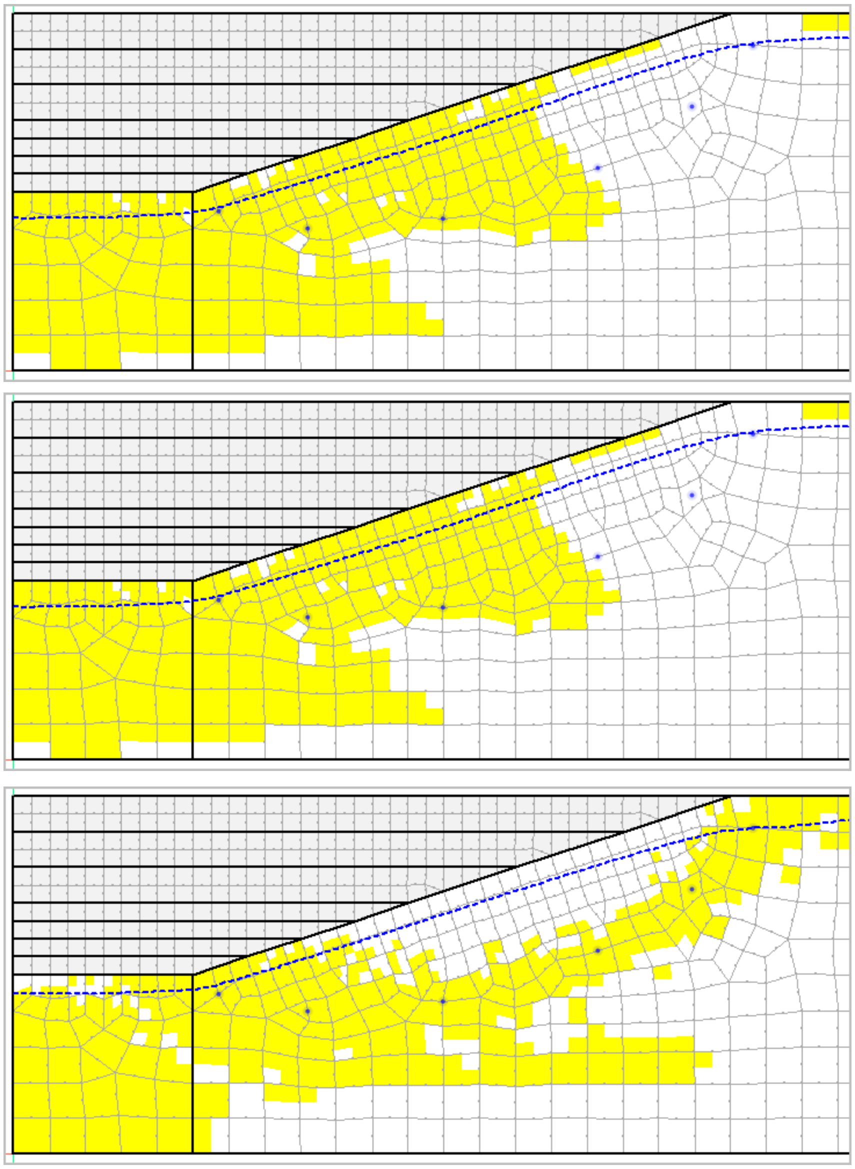

Figure 8. Extent of plastic (failure) zone after 11.3 year (top), 18.5 year (middle), and 30 year (bottom).

Figure 9 and Figure 10 show the variation of the effective cohesion and friction angle versus accumulated plastic deviatoric strain over the entire analysis. The graph locations are shown in Figure 8 and Figure 7 (bottom). Figure 11 isolates the data corresponding to an elapsed time of 18.5 years and reveals that strain softening had not initiated at the two locations nearest to the crest (Node 505/728). In fact, both points had a plastic deviatoric strain of zero 18.5 years, which means that the stress states had not even reached the peak strength failure envelop; consequently, the neighboring gauss regions are not all yellow in Figure 8 (middle). As such, a global rupture zone had not yet developed.

# GeoStudio Example - Progressive Failure of a Cut in London Clay due to Strain Softening

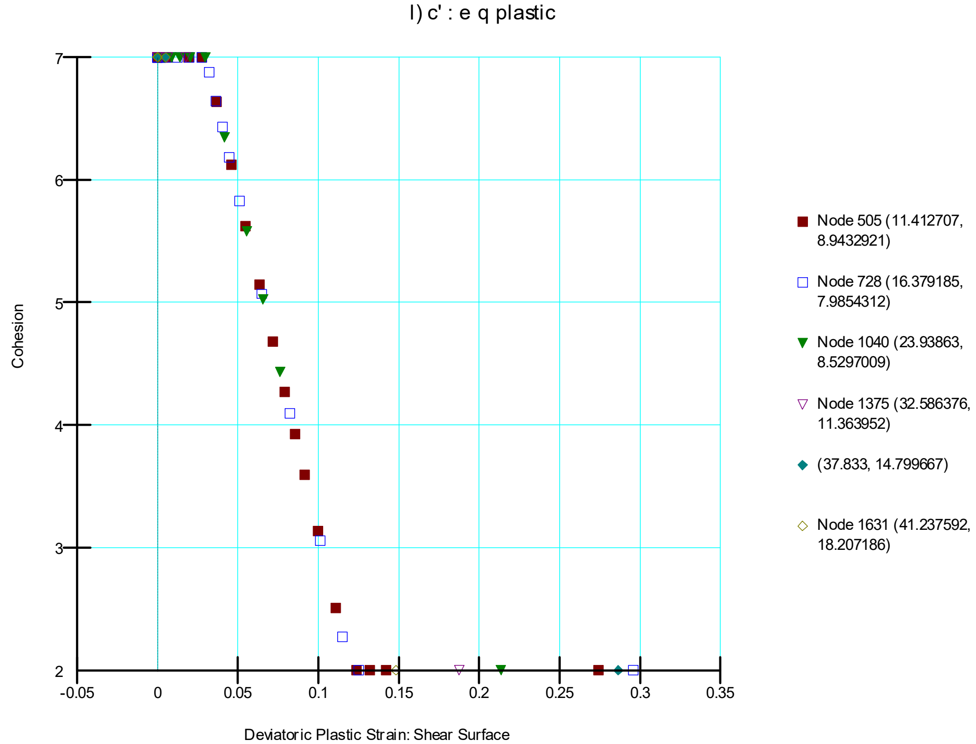


Figure 9. Simulated reduction in effective cohesion vs deviatoric plastic strain.

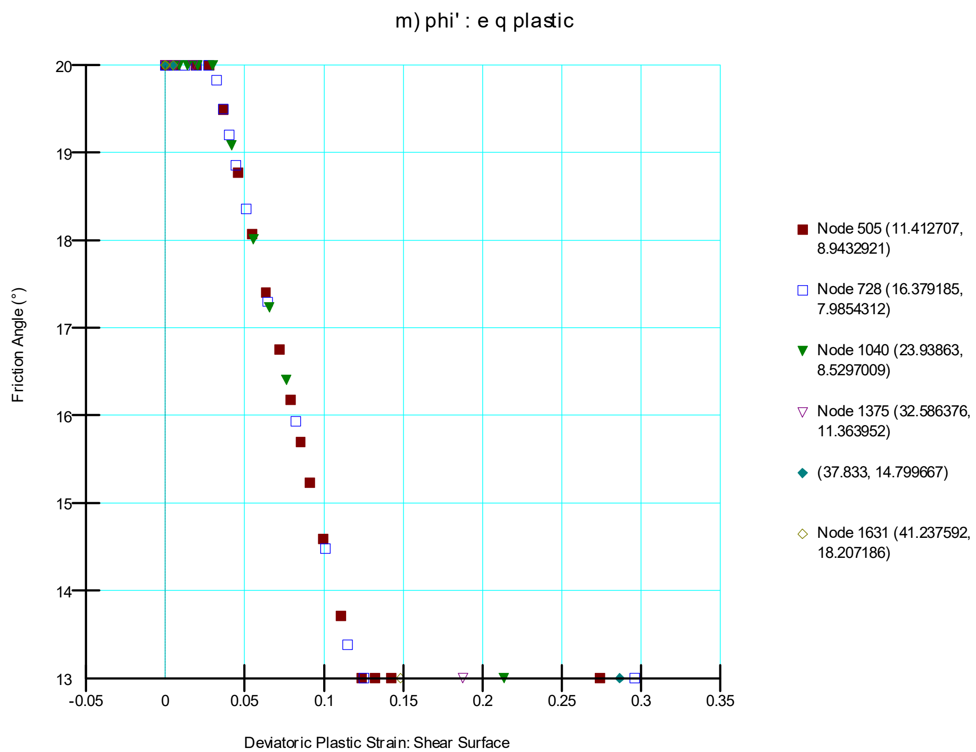


Figure 10. Simulated reduction in effective friction angle with deviatoric plastic strain.

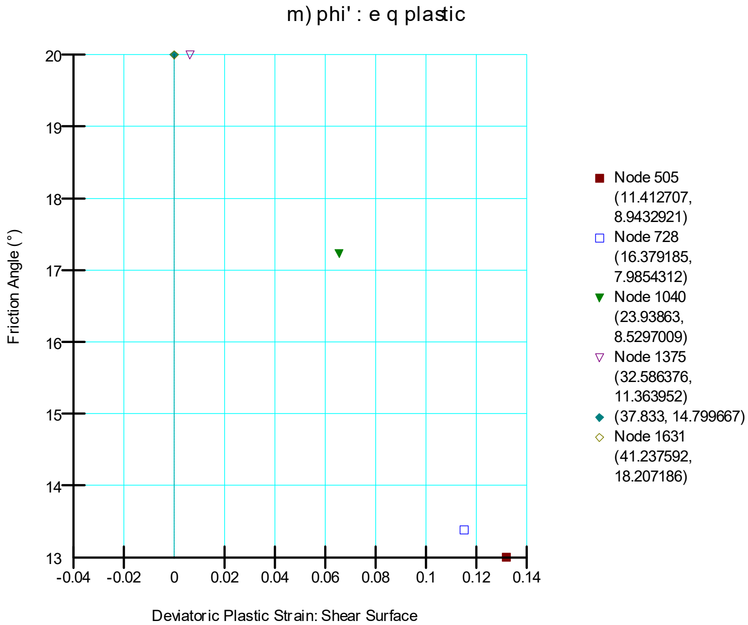


**Figure 11. Simulated reduction in friction angle with deviatoric plastic strain at elapsed time of 18.5.**

Figure 12 presents the displacement vectors overlaying the plastic deviatoric strain contours. The largest displacements are constrained within the rupture zone. One of the advantages of finite element stress-strain analyses is that there are no *a priori* kinematic constraints placed on the shape of the rupture zone. There are various other graphs in the associated project file that assist with interpretation of the results. Figure 13, for example, shows profiles of the lateral displacements at the toe of the slope. This graph shows that the deformations accelerated after 14.4 years (5276 days), suggesting that global failure was imminent at any time after this point in the slope's history. The exact timing of the failure is difficult to predict because the changes in the pore-water pressure are negligible after this point in time (5276 days; Figure 6).

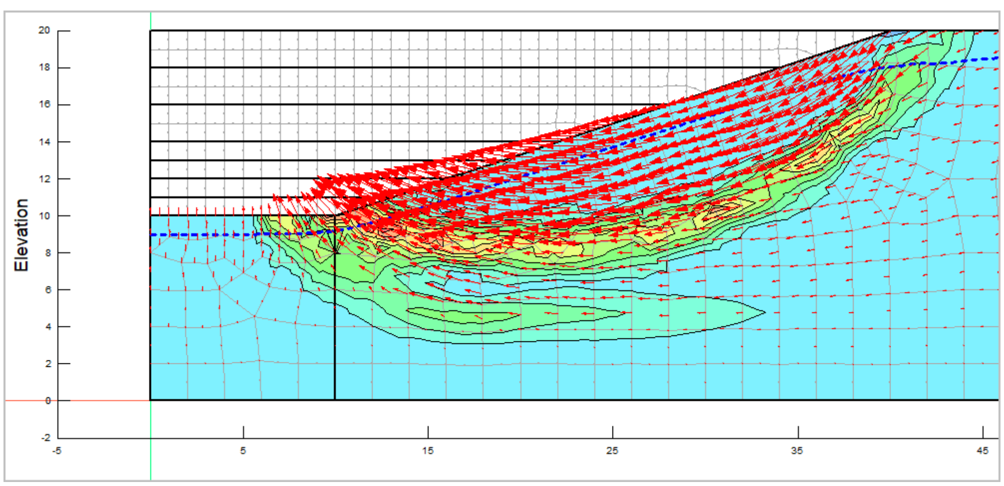


**Figure 12. Displacement vectors at 30 years.**

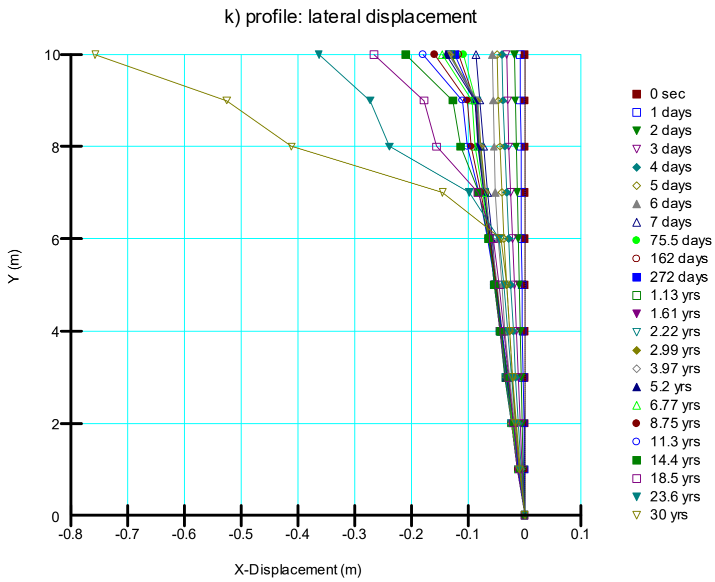


**Figure 13. Lateral displacement profile at the toe of the slope.**

The Relative Displacement/Residual Load scheme was used to determine convergence. (Seequent ULC, 2024). Although there are two measures of error, the relative displacement error controlled convergence in this analysis. The convergence tolerance was not met on the last three steps of the swelling analysis; however, the displacement error monotonically decreased towards the tolerable error on all steps (Figure 14). The relative residual force error provides additional insight into the evolution of the rupture zone despite not controlling convergence (Figure 15). The relative residual loads are oscillating with iteration instead of decreasing monotonically on the steps corresponding to 18.5 and 23.6 years. Once global rupture occurs, the residual loads increase with iteration on the last step, indicating that global equilibrium is unattainable. Additional refinement of time steps would be required to determine more precisely the onset of global failure.

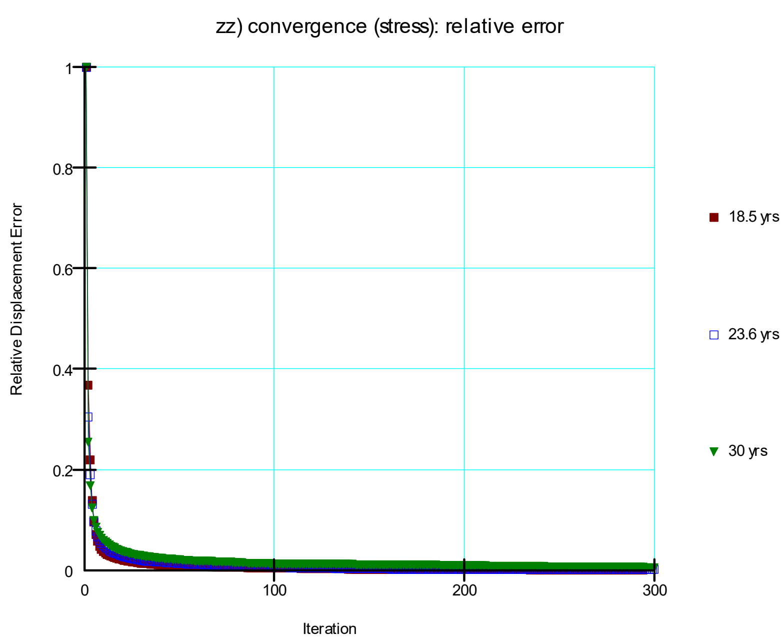

Figure 14. Relative displacement error vs iteration for the last 3 steps.

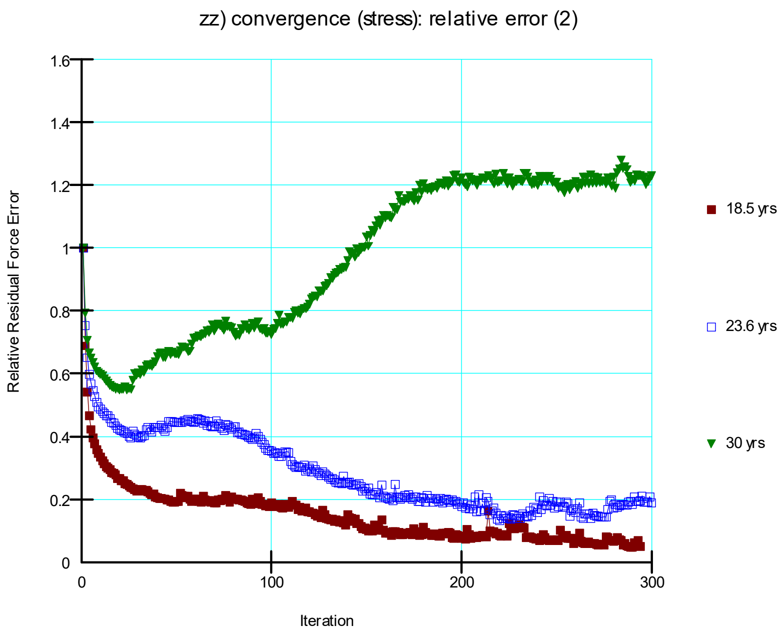


Figure 15. Relative residual force error vs iteration for the last 3 steps.

Potts et al. (1997) parameterized the material model differently than what was done in this study by considering various dilation angles and earth pressure coefficients, spatial variability in hydraulic conductivity, and stiffness variability with mean effective stress. The shape and evolution of the rupture zone varies slightly as a result of these additional considerations (Figure 16); however, the progressive failure mechanism was well represented in the SIGMA/W simulation despite the simplifying assumptions. Potts et al. (1997) carefully refined the time stepping to pinpoint the moment of global rupture to highlight the variation of strength along the rupture surface (Figure 16). The SIGMA/W swelling analysis can be completed in a similar manner by changing the time stepping sequence from exponential to linear and using 30 steps, which results in time steps of about 365.25 days.

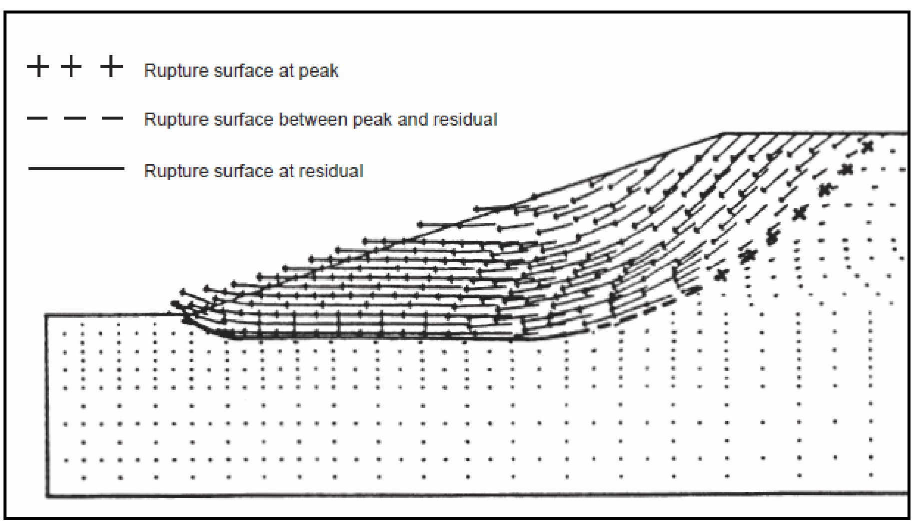


Figure 16. Strain softening failure surface from Potts et al. (1997).

## GeoStudio Example - Progressive Failure of a Cut in London Clay due to Strain Softening


# Summary

A Consolidation analysis, in combination with the Mohr-Coulomb Hardening/Softening material model, can be used to simulate a progressive failure mechanism. Progressive failure refers to the non-uniform mobilization of shear strength along a potential rupture surface. As illustrated by this example, a rupture zone can propagate from the toe to the crest of a cut slope as water pressures recover after an excavation. The rupture zone evolves because varying degrees of shear straining occur along a potential rupture zone. High shear zones experiences a reduction in strength, which simultaneously causes additional shear straining in other parts of the domain and therefore an associated decrease in strength. This mechanism is referred to as strain-softening. At collapse, part of the rupture surface will have a post-peak shear and perhaps approach a residual strength, while part of the rupture surface will not even have formed (Potts et al., 1997). An analysis of this type also provides information regarding the time to collapse.


# References


Griffiths, D.V. and Lane, P.A. (1999). Slope stability analysis by finite elements, Géotechnique, 49(3), 387-403.

Potts, D.M., Kovacevic, N., Vaughan, P.R. Delayed collapse of cut slopes in stiff clay. Géotechnique 47, No. 5, 953-982.

Seequent ULC. 2024. Stress-strain modeling with GeoStudio. Calgary, Alberta, Canada.